

## Dielectric properties of ultrathin SiO<sub>2</sub> slabs

N. Shi and R. Ramprasad<sup>a)</sup>

Department of Materials Science and Engineering, University of Connecticut, 97 N. Eagleville Road, Storrs, Connecticut 06269

(Received 17 August 2005; accepted 27 October 2005; published online 19 December 2005)

First-principles total energy calculations have been performed to determine the extent to which surfaces impact the dielectric properties of ultrathin dielectric materials. SiO<sub>2</sub> (0001) slabs in  $\alpha$ -quartz phase with various thicknesses were considered in this study, using a new method that allows for the partitioning of the surface and bulk contributions to the total field-induced polarization. It was found that the bulk polarization and the dielectric constant can be determined even from ultrathin films terminated with Si atoms, and that surface effects do not significantly impact the dielectric properties of (0001)  $\alpha$ -quartz slabs. © 2005 American Institute of Physics.  
[DOI: 10.1063/1.2150584]

In recent years, dielectric materials of nanoscale dimensions have aroused considerable interest. It is well known that the high-energy density capacitor industry is currently considering dielectric composites with a polymer host matrix filled with nanoplatelets of inorganic dielectric materials.<sup>1–5</sup> Also, for many present day microelectronics applications, thin-film morphologies are required.<sup>6,7</sup> In both of these cases, as the system sizes reach the nanoscale regime, polarization at the interfaces between the dielectric and other materials will be dominant in determining the dielectric properties. While several sophisticated first-principles methods have been employed to calculate the dielectric constant of bulk materials,<sup>8–13</sup> these methods do not allow for a practical characterization of such surface and interface effects. This letter comprises the initial steps aimed at an understanding of the extent to which such surface and interface effects modify the polarization and the dielectric constant of systems, using a new computationally efficient procedure.<sup>14</sup>

In this letter, first-principles density functional theory (DFT)-based calculations<sup>15</sup> are performed on SiO<sub>2</sub> in the  $\alpha$ -quartz phase. The dielectric properties of silicon-terminated slabs of  $\alpha$ -quartz along the (0001) direction are determined by establishing a connection with classical electrostatics, and a method to distinguish between the bulk and surface/interface contribution to the field-induced polarization is outlined. Our results indicate that the bulk contribution to the polarization (and the corresponding bulk dielectric constant) can be reliably extracted from these slab calculations, and that surfaces contribute negligibly to the total polarization for our choices of slabs.

All calculations were performed using the local density approximation within DFT (Ref. 15) as implemented in the local orbital SIESTA code.<sup>16</sup> Norm-conserving nonlocal pseudopotentials of the Troullier–Martins type were used to describe all the elements. The atomic configuration [Ne]3s<sup>2</sup>3p<sup>2</sup> was used for the Si pseudopotential and [He]2s<sup>2</sup>2p<sup>4</sup> for the O pseudopotential. A double-zeta plus polarization basis set was used for all calculations. 90 and 18 special **k** points, respectively, yielded well converged bulk and slab SiO<sub>2</sub> results. The equilibrium positions of the atoms were determined by requiring the forces on each atom to be

smaller than 0.04 eV/Å. Polarization due to an external electric field was studied using supercell slab calculations, as described earlier.<sup>14</sup>

$\alpha$ -quartz which occurs in a hexagonal crystal structure is the most widely studied and the most stable crystalline SiO<sub>2</sub> structure.<sup>17</sup> Figure 1 shows a schematic of the  $\alpha$ -quartz unit cell, which is completely defined by specifying the two lattice constants *a* and *c* as well as the four parameters—*u*, *x*, *y*, and *z*—which determine the internal coordinates of the three silicon and six oxygen atoms.<sup>18,19</sup> Our calculated structural properties of bulk  $\alpha$ -quartz are shown in Table I, and are in excellent agreement with experimental results.<sup>20</sup>

(0001)  $\alpha$ -quartz slabs, Si-terminated on both sides, composed of 2–13 Si planes were considered in this work. In the slab calculations, periodic boundary conditions were applied along the *x*-*y* directions parallel to the plane of the slab surfaces. These supercell calculations also involved the imposition of an artificial periodicity along the *z* direction perpendicular to the slab surface with sufficient vacuum separating the slab from its periodic images. For instance, a supercell thickness of ten times the equilibrium lattice constant along the *z* axis (54.136 Å) was used to determine the equilibrium

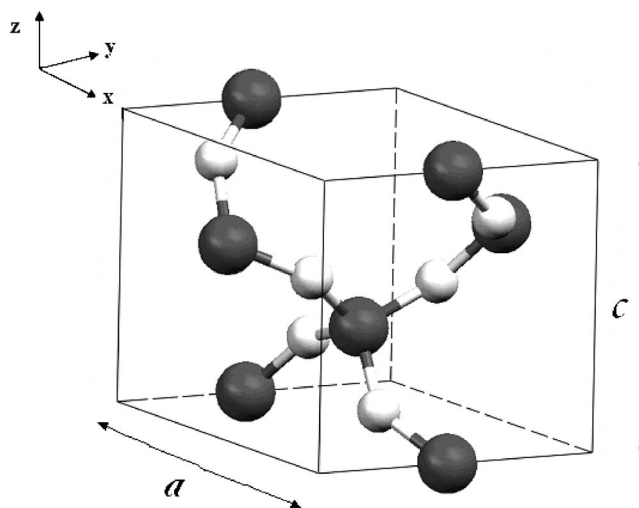


FIG. 1. Structure of the  $\alpha$ -quartz SiO<sub>2</sub> unit cell, with *a* and *c* being the lattice constants. White and black spheres represent O and Si atoms, respectively. Si atoms are at the face center sites of an external cube and O atoms at the simple cubic sites of an internal cube.

<sup>a)</sup>Electronic mail: rampi@ims.uconn.edu

TABLE I. Lattice constants ( $a$  and  $c$ ) in Å, and internal coordinates ( $u, x, y, z$ ) of  $\alpha$ -quartz.

	Theory	Expt. <sup>a</sup>
$a$	4.9099	4.9160
$c$	5.4136	5.4054
$u$	0.4641	0.4697
$x$	0.4016	0.4135
$y$	0.2720	0.2699
$z$	0.1101	0.1191

<sup>a</sup>See Ref. 20.

slab geometry in the absence of an external electric field. The calculated surface relaxations for all eight slabs are shown in Table II. The change of interlayer distances after relaxation is consistent with intuition and previous studies.<sup>21,22</sup> For all surfaces,  $\Delta d_{12}$  as defined in Table II is negative, corresponding to a reduction (compared to the bulk value) of the interlayer distance between the first and the second Si layers.  $\Delta d_{23}$  and  $\Delta d_{34}$ , where applicable, are relatively very small indicating that the surface relaxations are restricted to just the top two layers. The choices of these Si-terminated slabs were motivated by the fact that they have an intrinsic net dipole moment of zero in the absence of an electric field as explicitly ascertained by calculation.

In the next step, we exposed the slabs to an external electric field  $E_{\text{ext}}$  of 0.1 V/Å. The dipole moment per unit surface area of an isolated slab,  $m_0$ , induced due to the external applied field was calculated using a method described earlier.<sup>14</sup> The dipole moment as calculated by SIESTA is induced due to a combination of the external field and the spurious field due to the periodic image dipoles. It can be shown that the dipole moment calculated by SIESTA,  $m$ , is related to the true dipole moment of an isolated slab,  $m_0$ , by<sup>14</sup>

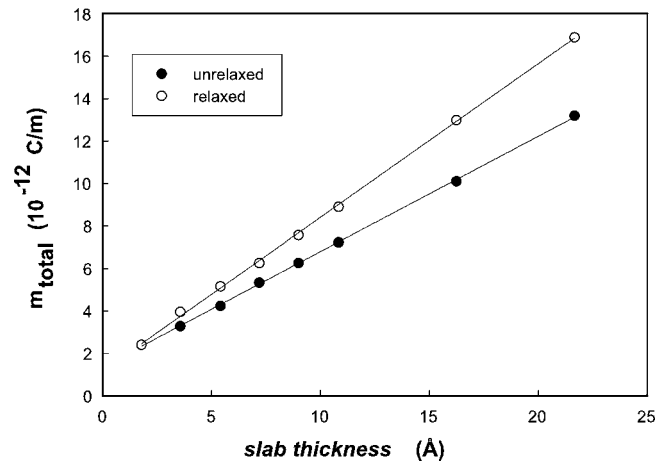
$$\frac{1}{m} = \frac{1}{m_0} - \left( \frac{1}{\epsilon_0 E_{\text{ext}}} \right) \frac{1}{L}, \quad (1)$$

where  $L$  is the supercell height or thickness perpendicular to the slab surface, and  $\epsilon_0$  and  $E_{\text{ext}}$  are the permittivity of free space and the external electric field, respectively. Thus, the intercept from a plot of the calculated  $1/m$  versus  $1/L$  for any given slab will yield the true field-induced dipole moment per unit area of the isolated slab.

Figure 2 shows a plot of  $m_0$  versus the slab thickness, both when the silicon and oxygen atoms were fixed at their

TABLE II. Surface relaxation in various slabs of  $\alpha$ -quartz.  $\Delta d_{ij} = (d_{ij} - d_0)/d_0$ , where  $d_{ij}$  is the distance along the  $z$  direction between Si atoms in the  $i$ th and  $j$ th planes, and  $d_0 = 1.8018$  Å is the corresponding distance in bulk  $\alpha$ -quartz.

No. of Si planes	$\Delta d_{12}$ (%)	$\Delta d_{23}$ (%)	$\Delta d_{34}$ (%)
2	-42.385	...	...
3	-20.276	...	...
4	-16.851	-2.838	...
5	-17.358	1.336	...
6	-17.536	1.434	0.010
7	-17.666	1.392	0.110
10	-17.631	0.568	-0.197
13	-17.631	0.598	-0.090

FIG. 2. Dependence of the total dipole moment density of an isolated  $\text{SiO}_2$  slab on the slab thickness.

field-free positions (indicated as “unrelaxed”), and when all atoms were allowed to move to their equilibrium positions in response to the applied electric field (indicated as “relaxed”).

From a classical point of view, we expect  $m_0$  to scale linearly with the thickness of the slab,  $t$ , with the bulk polarization given as  $m_0/t$ . However, atoms in the neighborhood of a surface or interface find themselves in chemically different environments compared to the bulk atoms due to changes in the coordination chemistry, oxidation states, and surface/interface relaxations. We thus expect the atomic species in the surface region to respond differently to an external electric field compared to the same species in the bulk region, allowing for a partitioning of the slab into surface and bulk regions. For thick enough slabs, a change in the total slab thickness translates to an equivalent change in the thickness of the bulk region, with the thickness of the surface region remaining the same. Consequently, we expect changes in  $m_0$  to scale linearly with changes in the slab thicknesses. The surface contribution to the total dipole moment, on the other hand, is not expected to depend on the thickness of the slab (for thick enough slabs). The above discussion does not hold for “thin” slabs that do not contain a sufficient amount of bulk region.

These intuitive notions are quantitatively realized for the  $\text{SiO}_2$  slabs considered here as shown in the plots of Fig. 2. We also observe an interesting behavior, similar to that seen in  $\text{HfO}_2$  slabs studied earlier.<sup>14</sup> Based on Table II, it is apparent that the surface relaxations are restricted to the top two layers, and that the correct values of the surface relaxations are recovered for slabs containing just five layers of Si planes (corresponding to a slab thickness of about 7.2 Å). This indicates that a minimum slab thickness of 7.2 Å is required to ensure the presence of a sufficiently thick bulk region. We thus expect a linear relationship between  $m_0$  and the slab thickness for slab thicker than 7.2 Å. While we do indeed see this expected behavior in Fig. 2 for both the relaxed and unrelaxed cases, we see only very slight departures from this linearity for slabs much thinner than 7.2 Å, indicating that even ultrathin  $\text{SiO}_2$  layers actually display bulk-like dielectric properties. As a reminder, we have considered only Si-terminated  $\text{SiO}_2$  slabs. Termination by other species, such as H, OH, and metal atoms, may cause the surface contribution to  $m_0$  (i.e., the intercept and small thickness behavior of the plots in Fig. 2) change drastically, thereby

altering the dielectric properties of such realistic thin-film situations.

The bulk polarization,  $P_{\text{bulk}}$ , obtained as the slope of the lines in Fig. 2 can be used to determine the bulk dielectric constant  $\epsilon$ , using:

$$\epsilon = \frac{\epsilon_0 E_{\text{ext}}}{\epsilon_0 E_{\text{ext}} - P_{\text{bulk}}}. \quad (2)$$

In the unrelaxed case of Fig. 2, only the distribution of the electrons was recalculated self-consistently after the application of the electric field, while all atoms were frozen at their field-free positions. This simulates the exposure of slabs to electric field with frequency high enough (e.g., optical) such that only the electrons are able to respond to the field. Using  $P_{\text{bulk}}$  corresponding to this situation would result in the electronic (or optical) part of the dielectric constant. Conversely, at low frequency or static fields, both the electrons and ions will respond to the external field. This is simulated by the relaxed case of Fig. 2, when both the electronic and ionic degrees of freedom are allowed to relax to their field-induced equilibrium situations. Using  $P_{\text{bulk}}$  corresponding to this case yields the total or static dielectric constant.

The calculated electronic and total dielectric constants using this method are 2.54 and 4.69 for  $\alpha$ -quartz, respectively, both of which compare very well with experimental results 2.40 and 4.52.<sup>23–26</sup>

In summary, we have used a new efficient method based on DFT for the calculation of the dielectric properties of ultrathin  $\alpha$ -quartz slabs. This method aids us in distinguishing between surface and bulk contributions to the total field-induced polarization. For the (0001)  $\alpha$ -quartz slabs considered here, the surface contribution to the dielectric properties is not significantly different from the bulk behavior. The bulk polarization and dielectric constant calculated using this method yield results in excellent agreement with experiments.

Partial support of this work by grants from the ACS Petroleum Research Fund and the Office of Naval Research is gratefully acknowledged.

- <sup>1</sup>J. Pyun and K. Matyjaszewski, *Chem. Mater.* **3436**, 13 (2001).
- <sup>2</sup>R. C. Advincula, *J. Dispersion Sci. Technol.* **24**, 343 (2003).
- <sup>3</sup>S. S. Ray and M. Okamoto, *Prog. Polym. Sci.* **28**, 1539 (2003).
- <sup>4</sup>Y. Rao and C. P. Wong, *J. Appl. Polym. Sci.* **92**, 2228 (2004).
- <sup>5</sup>S. O'Brian, L. Brus, and C. B. Murray, *J. Am. Chem. Soc.* **123**, 12085 (2001).
- <sup>6</sup>G. D. Wilk, R. M. Wallace, and J. M. Anthony, *J. Appl. Phys.* **89**, 5243 (2001).
- <sup>7</sup>A. I. Kingon, J. P. Maria, and S. K. Streiffer, *Nature (London)* **406**, 1032 (2000).
- <sup>8</sup>F. Detraux, P. Ghosez, and X. Gonze, *Phys. Rev. Lett.* **81**, 3297 (1998).
- <sup>9</sup>R. H. French, S. J. Glass, F. S. Ohuchi, Y. N. Xu, and W. Y. Ching, *Phys. Rev. B* **49**, 5133 (1994).
- <sup>10</sup>G.-M. Rignanese, F. Detraux, X. Gonze, and A. Pasquarello, *Phys. Rev. B* **64**, 134301 (2001).
- <sup>11</sup>X. Zhao and D. Vanderbilt, *Phys. Rev. B* **65**, 233106 (2002).
- <sup>12</sup>X. Zhao and D. Vanderbilt, *Phys. Rev. B* **65**, 075105 (2002).
- <sup>13</sup>R. D. King-Smith and D. Vanderbilt, *Phys. Rev. B* **47**, 1651 (1993).
- <sup>14</sup>R. Ramprasad and N. Shi, *Phys. Rev. B* **72**, 052107 (2005).
- <sup>15</sup>R. Martin, *Electronic Structure: Basic Theory and Practical Methods* (Cambridge University Press, New York, 2004).
- <sup>16</sup>J. M. Soler, E. Artacho, J. Gale, A. Garcia, J. Junquera, P. Ordejon, and D. Sanchez-Portal, *J. Phys.: Condens. Matter* **14**, 2745 (2002).
- <sup>17</sup>E. Chagarov, A. A. Demkov, and J. B. Adams, *Phys. Rev. B* **71**, 075417 (2005).
- <sup>18</sup>F. Liu and S. H. Garofalini, *Phys. Rev. B* **49**, 12528 (1994).
- <sup>19</sup>N. R. Keskar and J. R. Chelikowsky, *J. Phys.: Condens. Matter* **46**, 1 (1992).
- <sup>20</sup>L. Levien, C. T. Prewitt, and D. J. Weidner, *Mineral.* **65**, 140 (1983).
- <sup>21</sup>B. Meyer and D. Vanderbilt, *Phys. Rev. B* **63**, 205426 (2001).
- <sup>22</sup>M. Rarivomanantsoa, P. Jund, and R. Jullien, *J. Phys.: Condens. Matter* **13**, 6707 (2001).
- <sup>23</sup>W. L. Wolf, S. B. Stanley, and K. A. McCarthy, *American Institute of Physics Handbook* (McGraw-Hill, New York, 1963), p. 24.
- <sup>24</sup>F. Gervais and B. Piriou, *Phys. Rev. B* **11**, 3944 (1975).
- <sup>25</sup>W. G. Spitzer and D. A. Kleinman, *Phys. Rev.* **121**, 1324 (1961).
- <sup>26</sup>J. Fontanella, C. Andeen, and D. Schuele, *J. Appl. Phys.* **45**, 2852 (1974).